

# A Wideband Low-Profile Dual-Polarized Antenna Based on a Metasurface

Rui Wu <sup>1</sup>, Shuai Cao <sup>2</sup>, Yuan Liu <sup>1,\*</sup> and Shuting Cai <sup>1,\*</sup>

<sup>1</sup> School of Integrated Circuits, Guangdong University of Technology, Guangzhou 510006, China; wurui@gdut.edu.cn

<sup>2</sup> School of Automation, Guangdong University of Technology, Guangzhou 510006, China; 2112104379@mail2.gdut.edu.cn

\* Correspondence: eeliuyuan@gdut.edu.cn (Y.L.); shutingcai@gdut.edu.cn (S.C.)

**Abstract:** A wideband, low-profile, dual-polarized antenna using a metasurface (MS) is proposed in this paper. This design consists of a pair of crossed dipoles, an MS, a metal cavity and two baluns. The proposed MS acts as an artificial magnetic conductor (AMC), which is designed for the  $\pm 90^\circ$  reflection-phase bandwidth of 1.4–2.9 GHz. Compared with the  $0.25\lambda_0$  profile of the traditional crossed dipoles, the profile is reduced to  $0.15\lambda_0$  by using the in-phase reflection characteristics of the MS, which realizes the utilization of space. The measured results show that the antenna has a 10 dB return loss of 68.2% with isolation of more than 30 dB (1.45–2.95 GHz). The realized gain is 9 dBi with  $\pm 1$  dBi variation, especially exceeding 10 dBi from 2.1 to 2.8 GHz.

**Keywords:** wideband; low-profile; dual-polarized antenna; MS; AMC

## 1. Introduction

The rapid development of wireless communication systems has made dual-polarized antennas suitable for base stations. The wideband dual-polarized antenna can cover multiple wireless communication frequency bands, which satisfies the integration of wireless devices and effectively realizes the best interests of space. There are various approaches to improve the impedance bandwidth [1–10]. The Y-shaped feeding line helps to achieve a wide band [1,2]. The radiator is coupled with the parasitic element to form a multimode antenna, thereby expanding the operating frequency band [3–7]. In 2018, a novel dual-polarized multi-dipole antenna was proposed [7]. The radiator consists of a pair of big dipoles and a pair of small dipoles, achieving a wide band and stable radiation patterns. With the deepening of research, it has been found that an MS has the ability to achieve a wide band [8–13]. In 2022, a circularly polarized patch antenna using an MS achieved a 10 dB impedance bandwidth of 65.06% (5.62–11.04 GHz) [10].

The metal reflector has a fixed reflection phase of  $180^\circ$ . In order to achieve stable directional radiation, the distance between the antenna and the metal reflector is about a quarter of the wavelength. An artificial magnetic conductor (AMC), as a kind of MS, has the characteristics of in-phase reflection, which can be used to reduce profile and improve gain [14–22]. In [14], a circular AMC unit with in-phase reflection bandwidth of 2.4–2.7 GHz is proposed, which is combined with dipoles to achieve a height of  $0.08\lambda_0$  and a bandwidth of 22.3% (2.4–3 GHz). In [15], an AMC unit consisting of a circular patch and a ring is presented, operating in dual bands (2.33–2.57 GHz and 5–5.36 GHz). This antenna has a height of  $0.088\lambda_0$  at 2.4 GHz. In order to solve the problem of the AMC's narrow band, an AMC with a wide in-phase reflection band from 1.64 to 2.88 GHz is proposed in [16]. The antenna has a 10 dB impedance bandwidth of 54.8% and a low profile, but the gain is only 7.3 dBi with a variation of 0.7 dBi. It can be observed that the above AMCs reduce the profile, but the gain is not prominent and is lower than 8 dBi. The in-phase reflection property can be used to superimpose the reflected waves and the forward waves at an extremely low



**Citation:** Wu, R.; Cao, S.; Liu, Y.; Cai, S. A Wideband Low-Profile Dual-Polarized Antenna Based on a Metasurface. *Electronics* **2023**, *12*, 4739. <https://doi.org/10.3390/electronics12234739>

Academic Editor: Giovanni Crupi

Received: 31 October 2023

Revised: 17 November 2023

Accepted: 21 November 2023

Published: 22 November 2023



**Copyright:** © 2023 by the authors. Licensee MDPI, Basel, Switzerland. This article is an open access article distributed under the terms and conditions of the Creative Commons Attribution (CC BY) license (<https://creativecommons.org/licenses/by/4.0/>).

profile. The design in [17] has a gain of more than 9 dBi in the range of 3.6 to 5 GHz after using flower-type AMC. It is well known that microstrip antennas have the advantages of a low profile, small size and light weight, but the gain is not high [23,24]. However, in [25], using AMC achieves a wide band of 58.6% and a gain of more than 10 dBi across the entire operating band. The above published papers show that AMCs can not only reduce the profile, but also improve the gain. Modern communication systems require the antenna performance parameters to be balanced. In current society where spectrum resources are very precious, the number of users is increasing rapidly, and people's demand for transmission information is also constantly increasing. Multiple wireless communication systems need to be integrated into the same wireless device platform, which can effectively achieve the best use of space. Therefore, it is necessary to design an antenna with a wide band, low profile and high gain.

A wideband dual-polarized antenna with a low profile based on MS is presented in this paper. This design has a 10 dB impedance bandwidth of 68.2% from 1.45 to 2.95 GHz, covering the 2G (1710–1920 MHz), 3G (1880–2170 MHz) and 4G (2300–2400 and 2570–2690 MHz). An MS with a wide in-phase reflection phase band (1.45–2.93 GHz) is proposed. Combining the MS with the traditional crossed-dipoles, the antenna obtains a low profile of  $0.15\lambda_0$  ( $\lambda_0$  is free-space wavelength at the 2.2 GHz). The gain reaches  $9 \pm 1$  dBi in the whole operating band. It is worth noting that the antenna can achieve the superposition of reflected waves and forward waves at a low profile, resulting in gains above 10 dBi in the range of 2.1 to 2.7 GHz. With the aid of metallic walls and baluns for radiation pattern stability, low cross-polarization and a high front-to-back ratio are achieved over the operating frequency band.

## 2. Antenna Design and Analysis

### 2.1. Antenna Structure

The geometric configuration of the proposed antenna are shown in Figure 1. The antenna consists of a pair of crossed dipoles, an MS, a metal cavity and two baluns. The MS is a regularly arranged square lattices with slots printed on the FR4 substrate ( $\epsilon_r = 4.4$ ,  $\tan\delta = 0.02$ , and thickness of 0.8 mm). The radiation element is a pair of crossed dipoles printed on another FR4 substrate ( $\epsilon_r = 4.4$ ,  $\tan\delta = 0.02$ , and thickness of 0.8 mm). The metal cavity consists of a metallic ground and four metallic walls, which contribute to obtaining stable radiation patterns. The antenna has a height of  $0.15\lambda_0$  and is fed by  $50 \Omega$  coaxial lines. The optimized parameters are listed in Figure 1.

By comparing the performance of the four antennas in Figure 2, the structure of the proposed antenna is finally determined. Step 1 involves building a crossed-dipole antenna. The  $+45^\circ$  dipole is the driven dipole, and the  $-45^\circ$  dipole matches the  $50 \Omega$  load as the parasitic unit. The antenna produces two resonant modes. The first resonant mode is generated by the driven dipole, and the second is generated by the parasitic dipole due to strong coupling. Figure 2b shows that the frequency band of Ant.1 covers 1.7–3.1 GHz, but the gain is less than 8 dBi and the cross polarization is too large. The height of Ant. 1 is 38.8 mm ( $0.28\lambda_0$  at 2.2 GHz). In order to improve the radiation patterns and reduce the cross polarization, two baluns are added to Ant.1 in Step 2. Figure 2d shows that the cross polarization is reduced. It can be seen from Figure 2c that the gain is increased slightly. In Step 3, by introducing the MS, Ant. 3 achieves a low profile ( $20.8$  mm,  $0.15\lambda_0$ ) and a significant increase in gain. However, the cross polarization increases at 2.7 GHz. To solve the problem of excessive cross polarization of Ant. 3 at 2.7 GHz, four metallic walls are introduced. By comparison, the cross polarization of Ant. 4 is smaller than that of Ant. 3, and the impedance matching from 1.5 to 2.1 GHz is improved, and the gain is further enhanced.

Through the above four steps and the optimization of parameters, the structure of the proposed antenna was ultimately determined.  $\lambda_0$  is the free-space wavelength at the central frequency.

In order to improve the performance of antennas, it is necessary to study the parameters of MS. Therefore, the distance between the MS and the metallic ground ( $H_2$ ), the length of the slot ( $b$ ) and the gap ( $c$ ) are studied. When studying one of the parameters, the other parameters are kept as the values in Figure 1. Figure 3a shows that the increase in  $H_2$  causes the working band to move to lower frequencies, while improving impedance matching. Figure 3b illustrates that impedance matching is better when  $b$  is taken as 6 mm. As shown in Figure 3c, as  $c$  increases, the impedance matching deteriorates from 1.7 to 2.4 GHz, whereas the impedance matching gets better from 2.4 to 2.8 GHz.

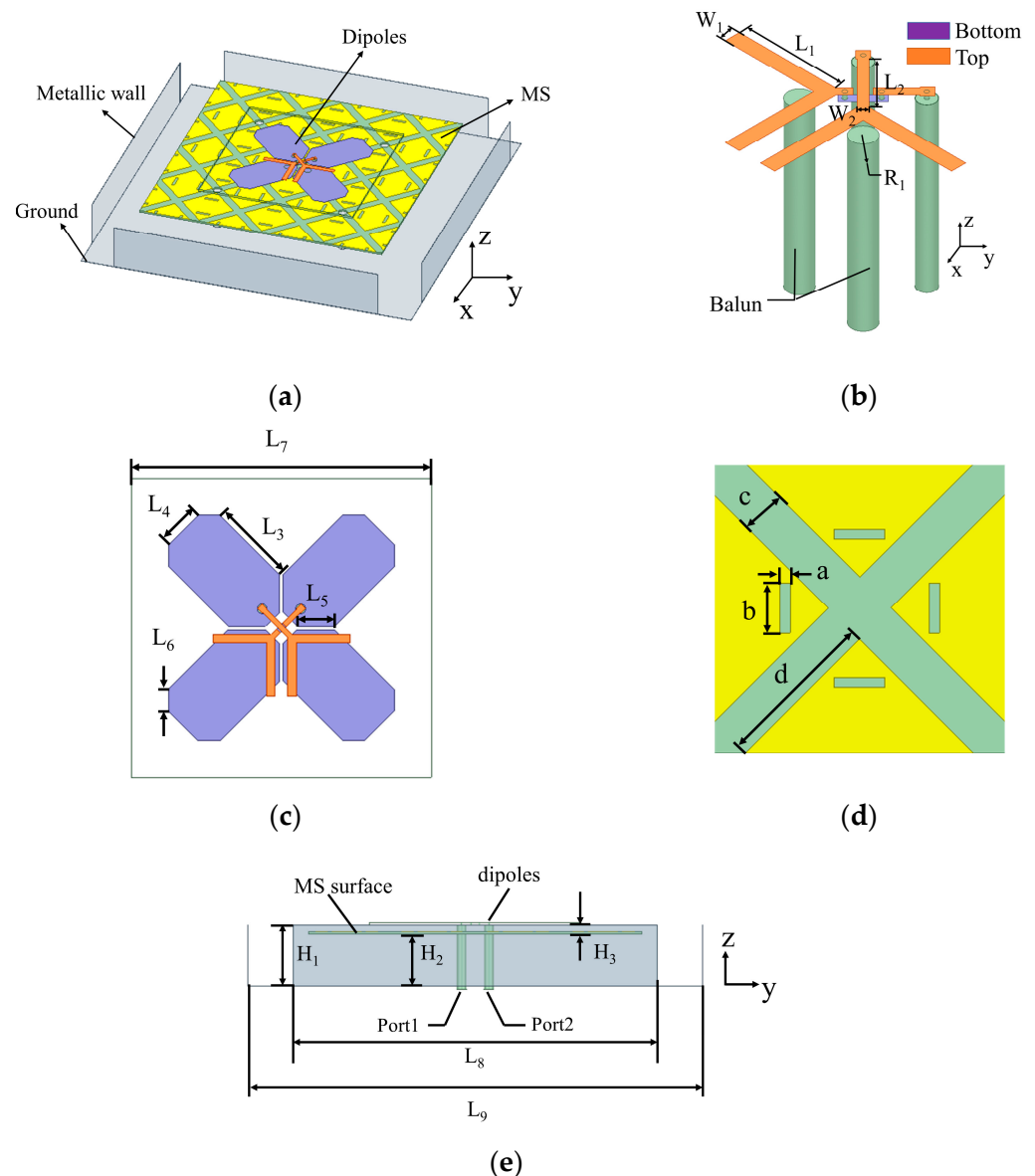


**Figure 1.** Configuration of the proposed antenna: (a) 3D view; (b) feeding structure. (c) top view of the dipoles; (d) top view of the MTS unit; (e) side view.  $L_1 = 13.7$ ;  $L_2 = 4.7$ ;  $L_3 = 19.8$ ;  $L_4 = 9.9$ ;  $L_5 = 8.7$ ;  $L_6 = 5$ ;  $L_7 = 70$ ;  $L_8 = 120$ ;  $L_9 = 150$ ;  $W_1 = 2$ ;  $W_2 = 1.2$ ;  $R_1 = 1.6$ ;  $H_1 = 20$ ;  $H_2 = 26$ ;  $H_3 = 8$ ;  $a = 1.2$ ;  $b = 6$ ;  $c = 3.5$ ;  $d = 16.5$ ; all in mm.

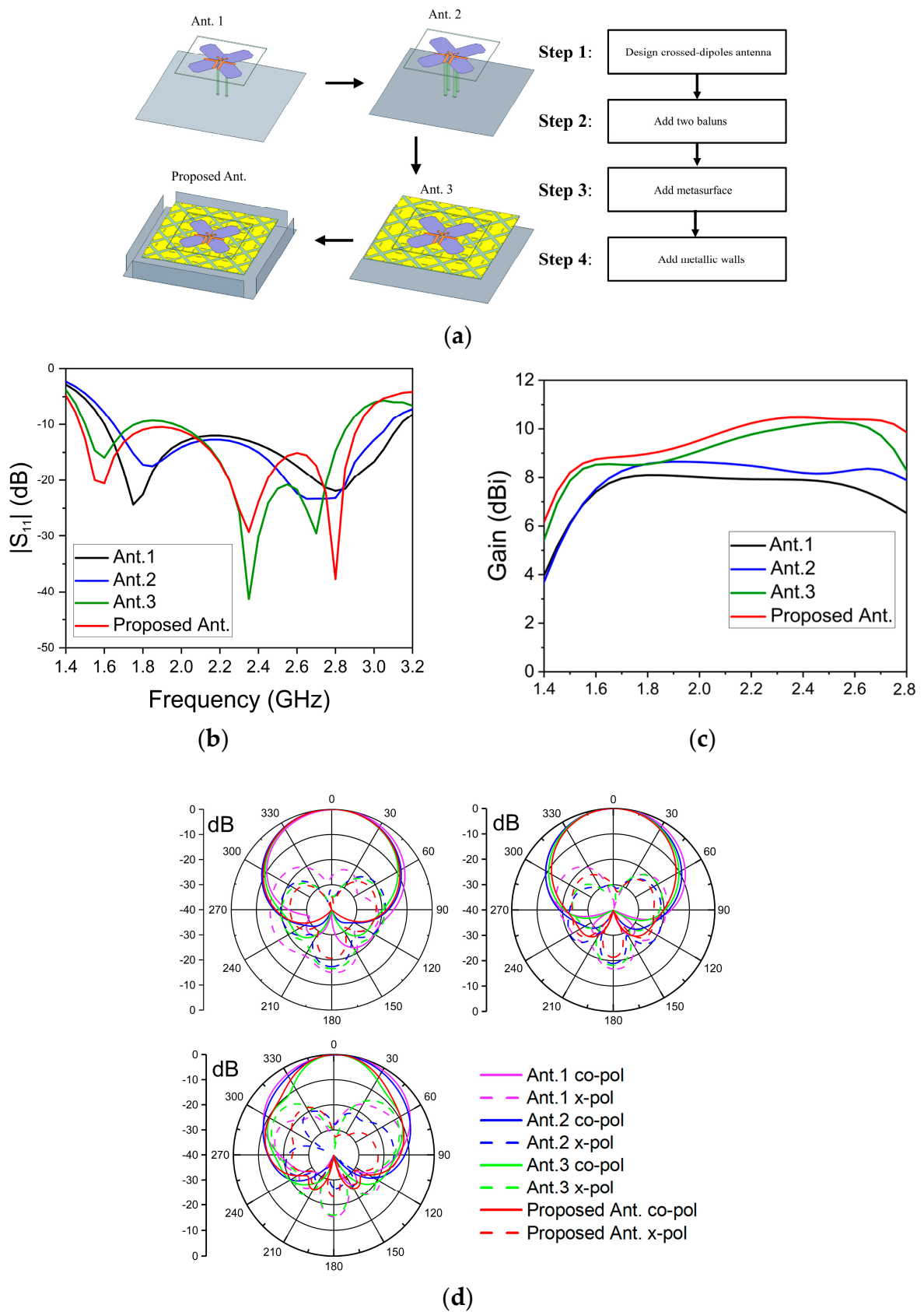


**Figure 2.** Performance comparison among four types of antennas: (a) Design steps of the proposed antenna, (b)  $|S_{11}|$ , (c) Gain, (d) Radiation patterns for xoz-plane.

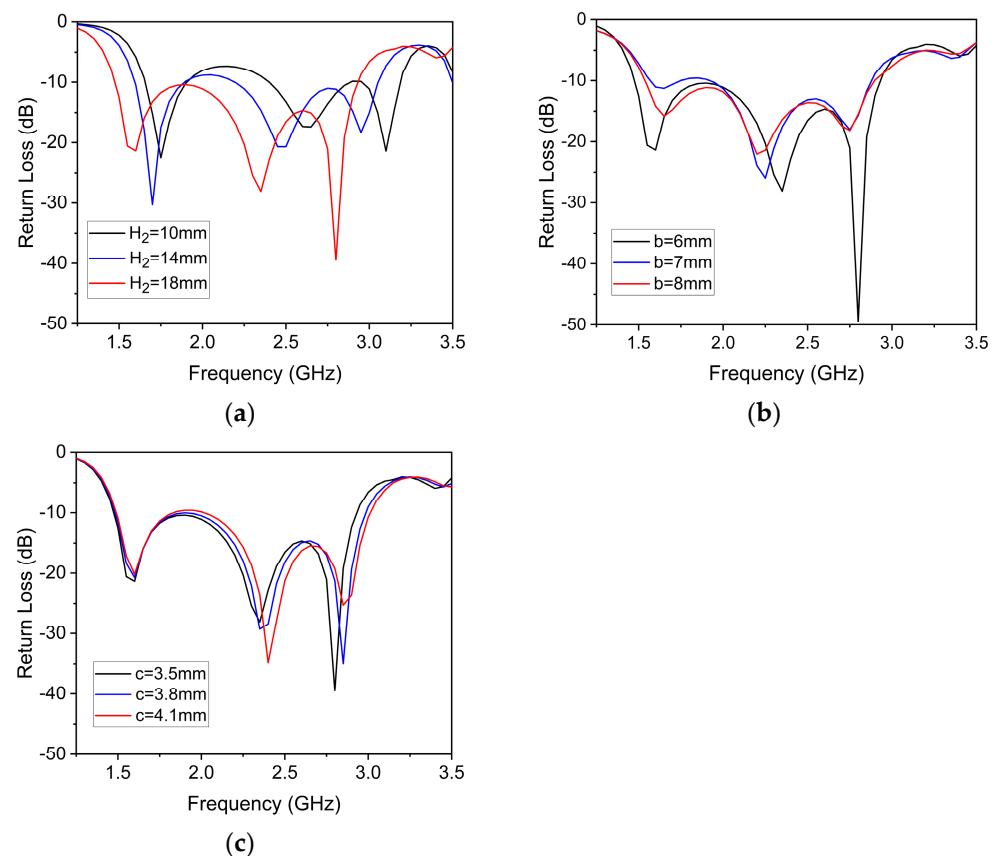


**Figure 3.** Analysis on the parameters of the MS: (a)  $H_2$ ; (b)  $b$ ; (c)  $c$ .

## 2.2. Design of MS Unit

An MS is a periodic structure, so it is only necessary to simulate a unit. By setting the matching port and boundary conditions, the electromagnetic characteristics of the infinite period MS structure can be simulated. At present, the methods of setting periodic boundary conditions include the Floquet Port method and the Wave Port method. In this paper, the Floquet Port method is used, and the specific modeling process is as follows:

- (1) Build an MS unit model and tightly attach it to the substrate to create an air box. The upper surface of the air box is at least  $\lambda/4$  from the upper patch of the MS unit, and the lower part of the FR4 substrate is set as a metal ground.
- (2) Set two pairs of master–slave boundaries on the four walls of the air box. The slave boundaries and their respective master boundaries are relative, and the vector direction of each pair of master–slave boundaries should be consistent.
- (3) Set the Floquet Port on the surface of the air box and use the Deembed function to move the port reference surface to the MS surface. Electromagnetic waves are incident from the Floquet Port and resonate on the MS surface, resulting in a reflection phase curve.

The MS proposed in this paper acts as an AMC. The proposed MS unit is shown in Figure 4, with an in-phase reflection band ranging from 1.45 to 2.93 GHz. The band with the reflection phase between  $+90^\circ$  and  $-90^\circ$  is the in-phase reflection band.

Four types of MS units are proposed here. By comparing the reflection phase curves, Figure 5 shows that the proposed MS unit has the widest in-phase reflection phase bandwidth, and the in-phase reflection bandwidth is improved after adding four slots.

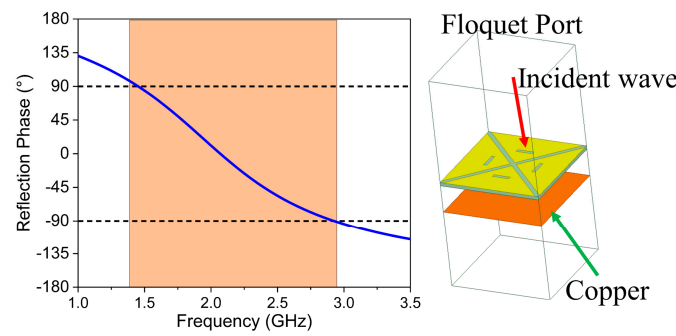


Figure 4. The reflection phase of the MS unit.

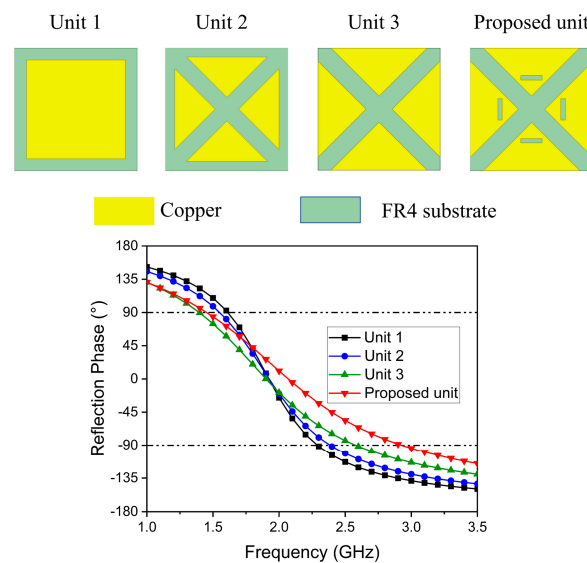
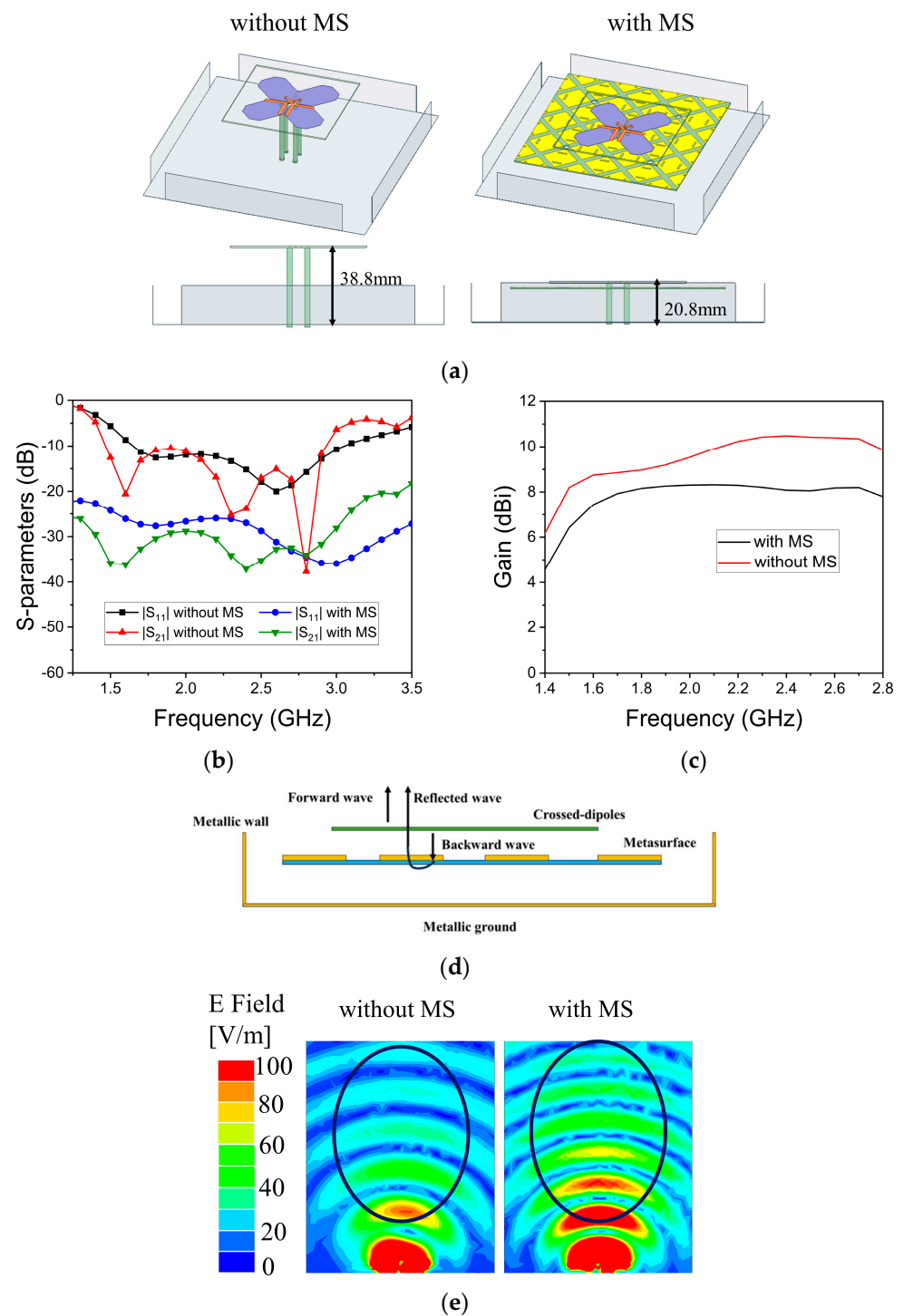


Figure 5. Four types of MS units and the reflection phase curves.

### 2.3. Effect of MS

The metallic reflector has a fixed  $180^\circ$  reflection phase, and it is necessary to introduce a quarter-wavelength profile, which greatly increases the size of the antenna. Figure 6a shows that the height is reduced from 38.8 mm to 20.8 mm by using the MS, almost half the original height. The profile of the antenna without an MS is  $0.28\lambda_0$  at 2.2 GHz, while the profile of the antenna with an MS is only  $0.15\lambda_0$  at 2.2 GHz. To show the effect of the MS, the S-parameters and gains of the proposed antenna are compared with those of antenna without an MS. As shown in Figure 6b, after using the MS, the band of the antenna moves to lower frequencies and the isolation is improved. The simulated results indicate that the bandwidth is 66.4% (1.47–2.93 GHz) and the isolation is greater than 30 dB. Figure 6c shows that the gain of the proposed antenna is higher than that of the antenna without an MS. It is worth noting that the gain is above 10 dBi in the range of 2.1 to 2.7 GHz. The mechanism of using the MS to enhance forward gain is shown in Figure 6d. The backward radiation electromagnetic waves are reflected by the MS and superimposed with the forward radiation electromagnetic waves, thereby enhancing the forward gain of the antenna. Figure 6e shows that the radiation of the antenna in the far field is enhanced, which indicates that the forward gain is enhanced.



**Figure 6.** Effects of MS: (a) 3D view of antennas with and without an MS; (b) simulated S-parameters; (c) simulated gain; (d) Schematic diagram of using the MS to enhance gain; (e) radiation field strength at 2.5 GHz for antennas with and without an MS.

### 3. Results

The prototype of the antenna is shown in Figure 7, and the final size is  $150 \times 150 \times 20.8 \text{ mm}^3$  ( $1.1 \times 1.1 \times 0.15\lambda_0^3$ ). Figure 8 shows that the measured results are basically consistent with the simulated results. Figure 8a shows the simulated and measured S-parameters. The antenna has a 10 dB impedance bandwidth of 68.2% from 1.45 to 2.95 GHz, with the isolation being greater than 30 dB. Figure 8b shows that the measured gain is  $9 \pm 1 \text{ dBi}$ . The measured gain is about 0.5 dBi lower than the simulated gain, which is normal. Due to the

superposition of the reflected waves and the forward waves, the gain of the antenna from 2.1 to 2.7 GHz is more than 10 dBi. Figure 8c shows that the antenna has stable radiation characteristics with stable radiation patterns. The front-to-back ratio (FBR) is greater than 20 dB and the cross-polarization discrimination (XPD) within  $\pm 60^\circ$  is greater than 10 dB. Due to the symmetrical structure, only the data for port 1 are provided.

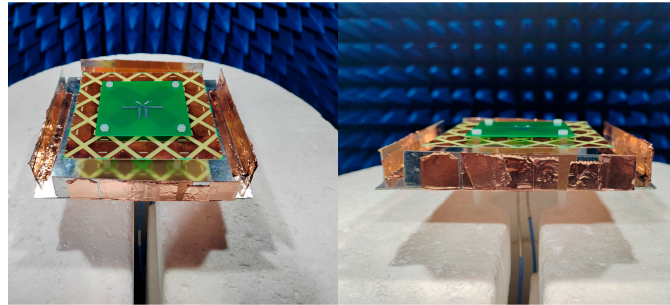


Figure 7. Prototype of the proposed antenna.

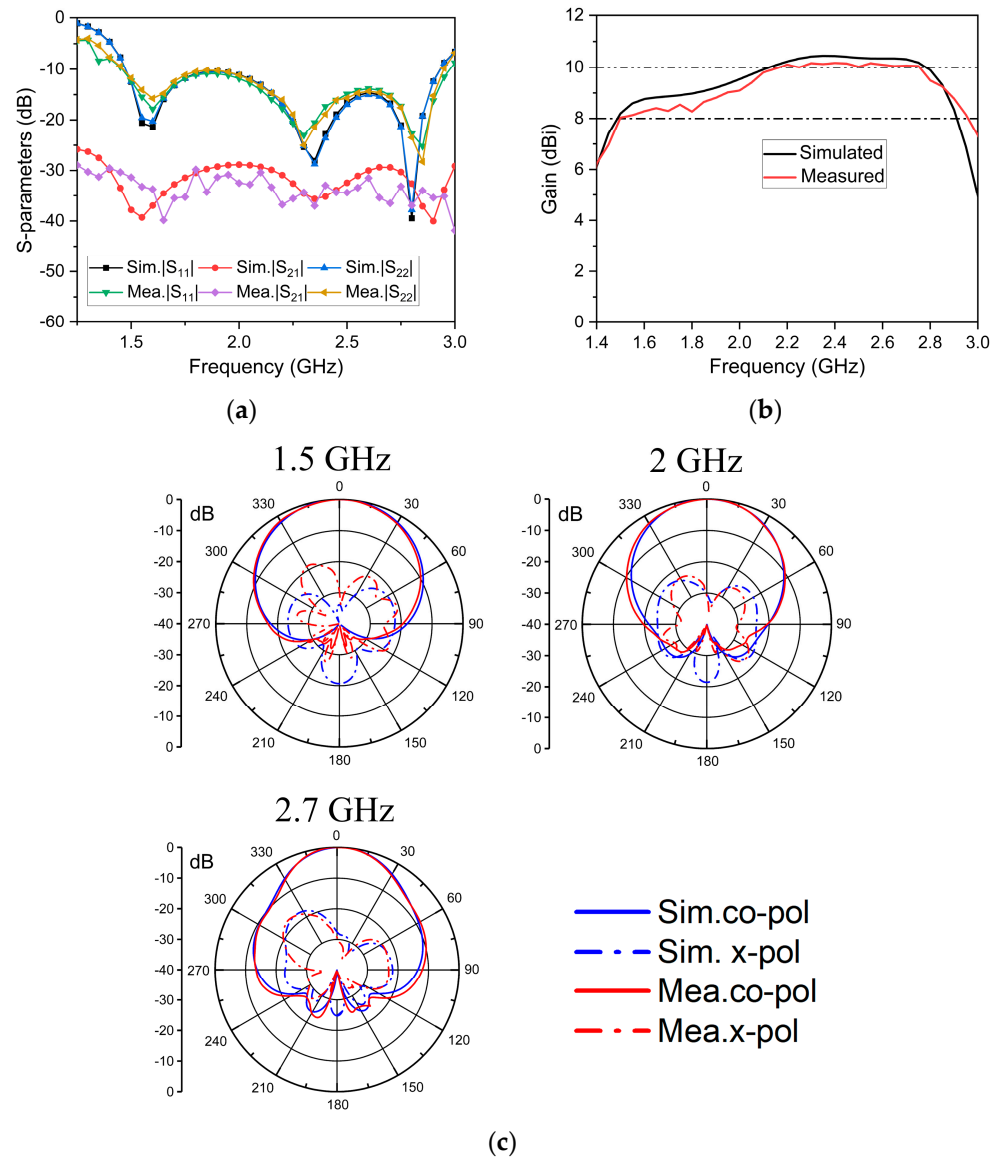


Figure 8. Measured and simulated results of the proposed antenna: (a) S-parameters; (b) gain; (c) radiation patterns at the XOZ plane.

The work in this paper is compared with some antennas using an MS in Table 1. By comparison, the bandwidth and isolation of this antenna are greater than those in Table 1, and the gain in the 4G band is greater than 10 dBi.

**Table 1.** Performance comparison with other antennas using MS.

Ref.	Bandwidth $ S_{11}  < -10$ dB	Gain (dBi)	Gain in 4G > 10 dBi	Isolation (dB)	Height ( $\lambda_0$ )
[13]	33% (0.69–0.96 GHz)	$8.3 \pm 0.9$	No	25	0.1
[14]	22.3% (2.4–3 GHz)	None	No	28	0.07
[16]	56.3% (1.63–2.87 GHz)	$7.3 \pm 0.7$	No	25	0.13
[22]	51.3% (1.68–2.84 GHz)	$8.8 \pm 0.4$	No	25	0.13
[26]	46.4% (1.69–2.71 GHz)	$9 \pm 1$	No	27	0.15
This work	68.2% (1.45–2.95 GHz)	$9.3 \pm 1.2$	Yes	30	0.15

$\lambda_0$ : Free-space wavelength at the center frequency.

#### 4. Conclusions

In this letter, a wideband dual-polarized antenna with a low profile has been proposed. Compared to the  $0.25\lambda_0$  profile of traditional crossed dipoles, this antenna utilizes the zero-reflection phase of the MS to achieve a low profile. The reflected electromagnetic waves and forward electromagnetic waves are superimposed in the same direction to enhance the gain, with a gain of over 10 dBi in the range of 2.1 to 2.7 GHz. The antenna structure is easy to manufacture and has good performance. It has good application prospects in future wireless systems.

**Author Contributions:** Conceptualization, R.W. and Y.L.; methodology, R.W.; software, S.C. (Shuai Cao); validation, S.C. (Shuting Cai), R.W. and S.C. (Shuai Cao); formal analysis, R.W. and S.C. (Shuting Cai); investigation, S.C. (Shuai Cao); resources, S.C. (Shuting Cai); data curation, S.C. (Shuai Cao); writing—original draft preparation, R.W. and S.C. (Shuai Cao); writing—review and editing, R.W., Y.L. and S.C. (Shuting Cai); visualization, R.W.; supervision, R.W.; project administration, Y.L. and S.C. (Shuting Cai); funding acquisition, R.W. All authors have read and agreed to the published version of the manuscript.

**Funding:** This research was funded by the National Nature Science Foundations of China (Grant No.: 61901176), in part by the Dean Project of Guangxi Wireless Broadband Communication and Signal Processing Key Laboratory (Grant No.: GXKL06220204), and in part by the Research and Development Project in Key Field of Guangdong Province, China (No. 2022B0701180001).

**Data Availability Statement:** Data can be requested from the author.

**Conflicts of Interest:** The authors declare no conflict of interest.

#### References

1. Wen, D.L.; Zheng, D.Z.; Chu, Q.X. A Dual-polarized Planar Antenna Using Four Folded Dipoles and Its Array for Base Stations. *IEEE Trans. Antennas Propag.* **2016**, *64*, 5536–5542. [\[CrossRef\]](#)
2. Chu, Q.X.; Wen, D.L.; Luo, Y. A Broadband  $\pm 45^\circ$  Dual-Polarized Antenna With Y-Shaped Feeding Lines. *IEEE Trans. Antennas Propag.* **2015**, *63*, 483–490. [\[CrossRef\]](#)
3. Li, J.; Hao, S.J.; Cui, Y.G.; Chen, X. A Miniaturized Wideband Dual-Polarized Planar Antenna Based on Multiresonance. *IEEE Antennas Wirel. Propag. Lett.* **2022**, *21*, 242–246. [\[CrossRef\]](#)
4. Wu, R.; Xue, Q.; Chu, Q.X.; Chen, F.C. Ultrawideband Dual-Polarized Antenna for LTE600/LTE700/GSM850/GSM900 Application. *IEEE Antennas Wirel. Propag. Lett.* **2021**, *20*, 1135–1139. [\[CrossRef\]](#)
5. Yang, W.; Pan, Y. A Wideband Dual-Polarized Dipole Antenna with Folded Metallic Plates. *IEEE Antennas Wirel. Propag. Lett.* **2018**, *17*, 1797–1801. [\[CrossRef\]](#)
6. Luo, Y.; Chu, Q.X. Oriental Crown-Shaped Differentially Fed Dual-Polarized Multidipole Antenna. *IEEE Trans. Antennas Propag.* **2015**, *63*, 4678–4685. [\[CrossRef\]](#)
7. Chen, Y.; Lin, W.; Li, S.; Raza, A. A Broadband  $\pm 45^\circ$  Dual-Polarized Multidipole Antenna Fed by Capacitive Coupling. *IEEE Trans. Antennas Propag.* **2018**, *66*, 2644–2649. [\[CrossRef\]](#)

8. Liu, S.; Yang, D.; Chen, Y.; Sun, K.; Zhang, X.; Xiang, Y. Low-Profile Broadband Metasurface Antenna Under Multimode Resonance. *IEEE Antennas Wirel. Propag. Lett.* **2021**, *20*, 1696–1700. [[CrossRef](#)]
9. Wang, J.; Wong, H.; Ji, Z.; Wu, Y. Broadband CPW-Fed Aperture Coupled Metasurface Antenna. *IEEE Antennas Wirel. Propag. Lett.* **2019**, *18*, 517–520. [[CrossRef](#)]
10. Kedze, K.E.; Wang, H.; Park, I. A Metasurface-Based Wide-Bandwidth and High-Gain Circularly Polarized Patch Antenna. *IEEE Trans. Antennas Propag.* **2022**, *70*, 732–737. [[CrossRef](#)]
11. Liu, G.; Sun, X.; Chen, X.; Xiong, D.; Li, M.; Tang, M.C. A Broadband Low-Profile Dual-Linearly Polarized Dipole-Driven Metasurface Antenna. *IEEE Antennas Wirel. Propag. Lett.* **2020**, *19*, 1759–1763. [[CrossRef](#)]
12. Liu, W.E.I.; Chen, Z.N.; Qing, X.; Shi, J.; Lin, F.H. Miniaturized Wideband Metasurface Antennas. *IEEE Trans. Antennas Propag.* **2017**, *65*, 7345–7349. [[CrossRef](#)]
13. Zhu, H.; Qiu, Y.; Wei, G. A Broadband Dual-Polarized Antenna with Low Profile Using Nonuniform Metasurface. *IEEE Antennas Wirel. Propag. Lett.* **2019**, *18*, 1134–1138. [[CrossRef](#)]
14. Zhai, H.; Xi, L.; Zang, Y.; Li, L. A Low-Profile Dual-Polarized High-Isolation MIMO Antenna Arrays for Wideband Base-Station Applications. *IEEE Trans. Antennas Propag.* **2018**, *66*, 191–202. [[CrossRef](#)]
15. Zhai, H.; Zhang, K.; Yang, S.; Feng, D. A Low-Profile Dual-Band Dual-Polarized Antenna with an AMC Surface for WLAN Applications. *IEEE Antennas Wirel. Propag. Lett.* **2017**, *16*, 2692–2695.
16. Li, M.; Li, Q.L.; Wang, B.; Zhou, C.F.; Cheung, S.W. A Low-Profile Dual-Polarized Dipole Antenna Using Wideband AMC Reflector. *IEEE Trans. Antennas Propag.* **2018**, *66*, 2610–2615. [[CrossRef](#)]
17. Wang, B.; Liao, C.; Du, C.H. A Low-Profile Broadband Dual-Polarized Base Station Antenna Array with Well-Suppressed Cross-Polarization. *IEEE Trans. Antennas Propag.* **2021**, *69*, 8354–8365. [[CrossRef](#)]
18. Zhu, J.; Li, S.; Liao, S.; Xue, Q. Wideband Low-Profile Highly Isolated MIMO Antenna with Artificial Magnetic Conductor. *IEEE Antennas Wirel. Propag. Lett.* **2018**, *17*, 458–462. [[CrossRef](#)]
19. Tran, H.H.; Park, I. A Dual-Wideband Circularly Polarized Antenna Using an Artificial Magnetic Conductor. *IEEE Antennas Wirel. Propag. Lett.* **2016**, *15*, 950–953. [[CrossRef](#)]
20. Nie, Z.; Zhai, H.; Liu, L.; Li, J.; Hu, D.; Shi, J. A Dual-Polarized Frequency-Reconfigurable Low-Profile Antenna with Harmonic Suppression for 5G Application. *IEEE Antennas Wirel. Propag. Lett.* **2019**, *18*, 1228–1232. [[CrossRef](#)]
21. Yang, S.; Liang, L.; Wang, W.; Fang, Z.; Zheng, Y. Wideband Gain Enhancement of an AMC Cavity-Backed Dual-Polarized Antenna. *IEEE Trans. Veh. Technol.* **2021**, *70*, 12703–12712. [[CrossRef](#)]
22. Zhou, C.; Sun, J.; Yang, W.W.; Li, M.; Wong, H. A Wideband Low-Profile Dual-Polarized Hybrid Antenna Using Two Different Modes. *IEEE Antennas Wirel. Propag. Lett.* **2023**, *22*, 114–118. [[CrossRef](#)]
23. Leonardi, O.; Pavone, M.G.; Sorbello, G.; Morabito, A.F.; Isernia, T. Compact single-layer circularly polarized antenna for short-range communication systems. *Microw. Opt. Technol. Lett.* **2014**, *56*, 1843–1846. [[CrossRef](#)]
24. Mauro, G.S.; Castorina, G.; Morabito, A.F.; Di Donato, L.; Sorbello, G. Effects of lossy background and rebars on antennas embedded in concrete structures. *Microw. Opt. Technol. Lett.* **2016**, *58*, 2653–2656. [[CrossRef](#)]
25. Ntawangaheza, J.d.D.; Sun, L.; Yang, C.; Pang, Y.; Rushingabigwi, G. Thin-Profile Wideband and High-Gain Microstrip Patch Antenna on a Modified AMC. *IEEE Antennas Wirel. Propag. Lett.* **2019**, *18*, 2518–2522.
26. Syed Nasser, S.S.; Chen, Z.N. Low-Profile Broadband Dual-Polarization Double-Layer Metasurface Antenna for 2G/3G/LTE Cellular Base Stations. *IEEE Trans. Antennas Propag.* **2022**, *70*, 75–83. [[CrossRef](#)]

**Disclaimer/Publisher’s Note:** The statements, opinions and data contained in all publications are solely those of the individual author(s) and contributor(s) and not of MDPI and/or the editor(s). MDPI and/or the editor(s) disclaim responsibility for any injury to people or property resulting from any ideas, methods, instructions or products referred to in the content.